

*Supporting Information*

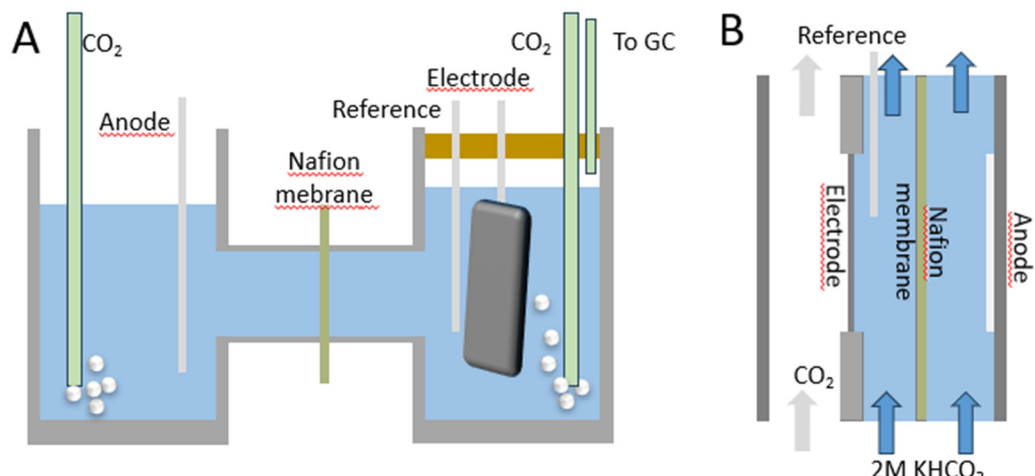
# Effects of Annealing Conditions on the Catalytic Performance of Anodized Tin Oxide for Electrochemical Carbon Dioxide Reduction

Nicolò B. D. Monti <sup>1,2</sup>, Juqin Zeng <sup>1,2,\*</sup>, Micaela Castellino <sup>1,2</sup>, Samuele Porro <sup>2</sup>, Mitra Bagheri <sup>1,2</sup>, Candido F. Pirri <sup>1,2</sup>, Angelica Chiodoni <sup>1</sup> and Katarzyna Bejtka <sup>1,2,\*</sup>

<sup>1</sup> Center for Sustainable Future Technologies @POLITO, Istituto Italiano di Tecnologia, Via Livorno 60, 10144 Turin, Italy

<sup>2</sup> Department of Applied Science and Technology, Politecnico di Torino, C.so Duca degli Abruzzi 24, 10129 Turin, Italy

\* Correspondence: juqin.zeng@polito.it (J.Z.); katarzyna.bejtka@polito.it (K.B.)



Academic Editor: George Z. Kyzas

Received: 31 December 2024

Revised: 11 January 2025

Accepted: 13 January 2025

Published: 16 January 2025

**Citation:** Monti, N.B.D.; Zeng, J.; Castellino, M.; Porro, S.; Bagheri, M.; Pirri, C.F.; Chiodoni, A.; Bejtka, K. Effects of Annealing Conditions on the Catalytic Performance of Anodized Tin Oxide for Electrochemical Carbon Dioxide Reduction. *Nanomaterials* **2025**, *15*, 121. <https://doi.org/10.3390/nano15020121>

**Copyright:** © 2025 by the authors. Licensee MDPI, Basel, Switzerland. This article is an open access article distributed under the terms and conditions of the Creative Commons Attribution (CC BY) license (<https://creativecommons.org/licenses/by/4.0/>).

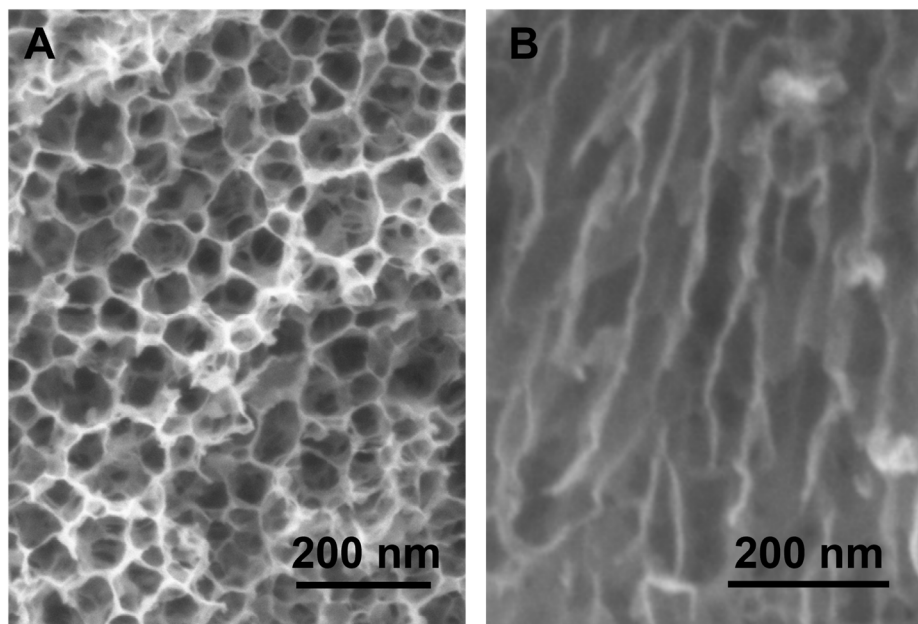


**Figure S2.** FESEM images of pristine catalyst: (A) top view and (B) cross-section view.

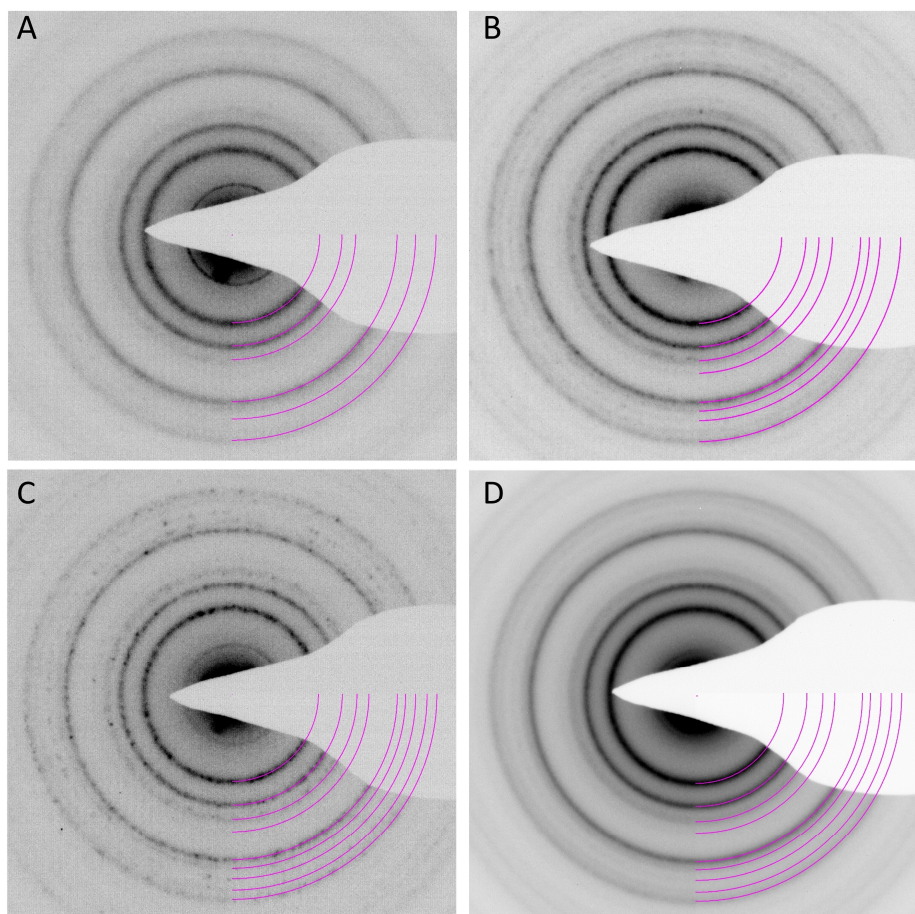


**Figure S3.** Selected Area Electron Diffraction (SAED) patterns of all studied catalysts: (A) Pristine, (B) Air'-370deg, (C) Air'-525deg and (D) N2'-525deg. The rings in the images were obtained by Circular Hough transform diffraction analysis (A software tool for automated measurement of selected area electron diffraction patterns within Digital Micrograph [1]), and are superimposed on the SAED pattern, showing the position and size of the rings. These are polycrystalline SnO<sub>2</sub> (Tin Oxide, JCPDS 00-041-1445).

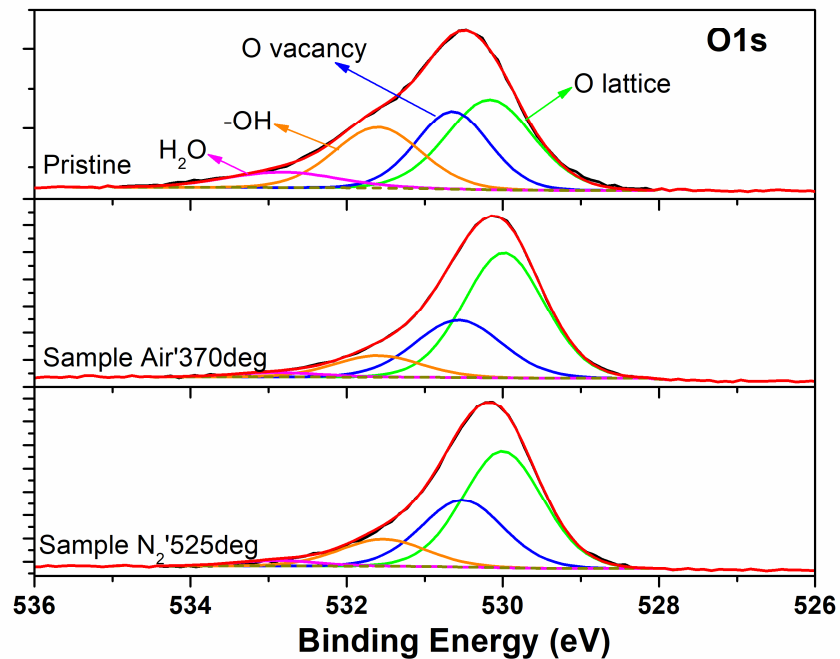


**Figure S4.** XPS O1s HR spectra for pristine, annealed in air at 370 °C and annealed in inert atmosphere at 525 °C.

**Table S1.** O 1s XPS peak deconvolution results for the four samples.

Samples	O1s XPS peak deconvolution results			
	Lattice O	O <sub>vac</sub>	-OH	H <sub>2</sub> O
Pristine	38.1	27.8	25.7	8.4
Air'370°C	58.5	28.5	10.7	2.3
Air'525°C	53.1	31.2	13.2	2.5
N <sub>2</sub> '525°C	54.9	27.4	14.3	3.4

**Table S2.** Comparison of Electrocatalytic Performance of Tin-Based Catalysts for CO<sub>2</sub> Reduction to Formic Acid / formate and CO.

Electrocatalysts	Electrolyte	FE <sub>CO<sub>2</sub></sub> RR [%]	Applied potential [V vs. RHE]	Current density [mA cm <sup>-2</sup> ]	Stability [h]	Ref
Mesoporous SnO <sub>x</sub> Nanoparticles	2 M KHCO <sub>3</sub>	95	-1.2	72	30	This work
Wavy SnO <sub>2</sub>	0.5 M KHCO <sub>3</sub>	91	-1.0	22 S	18	[2]
Mesoporous SnO <sub>2</sub> nanosheets	0.5 M KHCO <sub>3</sub>	90	-1.3	8.3	12	[3]
Porous SnO <sub>2</sub> /CC	0.5 M NaHCO <sub>3</sub>	95	-1.6 (V vs. Ag/AgCl)	45	24	[4]
Porous SnO <sub>2</sub> nanosheets	0.5 M KHCO <sub>3</sub>	92.4	-0.7	NA	10	[5]
Ultra-small SnO <sub>2</sub> NPs	1 M KHCO <sub>3</sub>	80	-1.21	145	NA	[6]
Ultrathin SnO <sub>2</sub> QWs	0.1 M KHCO <sub>3</sub>	87.3	-1.156	13.7	7	[7]
Pt atom/SnO <sub>2</sub>	0.1 M KHCO <sub>3</sub>	82.1 ± 1.4	-1.2	12.9	8	[8]
In-SnO <sub>2</sub> NWs	0.5 M KHCO <sub>3</sub>	85	-1.04	6.02	12	[9]
Mn-doped SnO <sub>2</sub>	0.1 M KHCO <sub>3</sub>	91.6	-1.03	21.2	8	[10]
VO-rich N-SnO <sub>2</sub> NS	0.1 M KHCO <sub>3</sub>	>90	-0.9	6.7	10	[11]
SnO <sub>2</sub> @N-CNW	0.5 M NaHCO <sub>3</sub>	90	-0.8	25	20	[12]
NC-SnO <sub>2</sub> @CC	0.5 M KHCO <sub>3</sub>	93	-0.7	44.3	24	[13]
SnO <sub>2</sub> /Sn	0.5 M KHCO <sub>3</sub>	93 ± 1	-1.0	28.7	9	[14]
SnO <sub>2</sub> /Py-CNTO	0.1 M KHCO <sub>3</sub>	96	-1.29	27.5	32	[15]

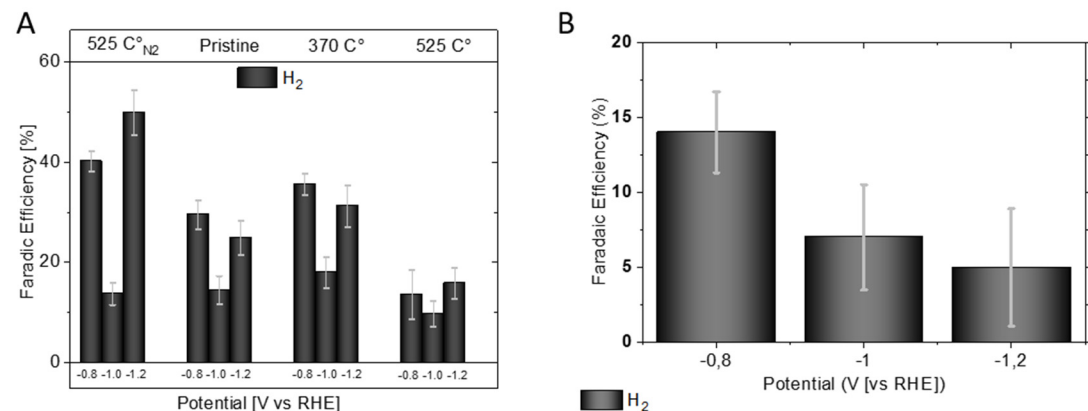


**Figure S5.** FE of H<sub>2</sub> of: A) H-cell experiments and B) flow cell experiments.

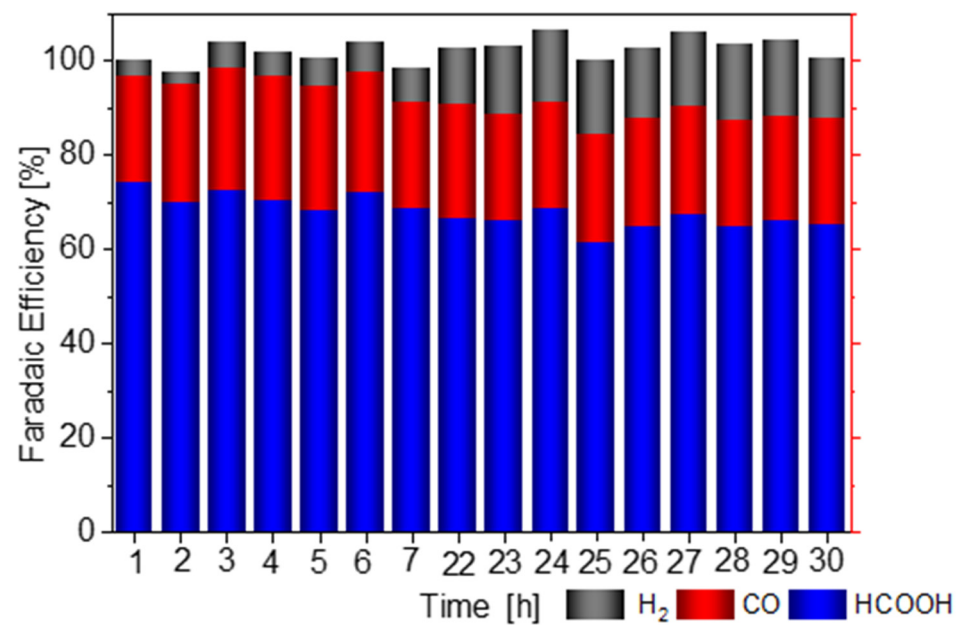


**Figure S6.** Stability test complete FE distribution at sampling time.

## REFERENCES

1. D.R.G. Mitchell, Circular Hough transform diffraction analysis: A software tool for automated measurement of selected area electron diffraction patterns within Digital MicrographTM, Ultramicroscopy 108 (2008) 367–374.  
<https://doi.org/10.1016/j.ultramic.2007.06.003>.

2. Z. Chen, T. Fan, Y.Q. Zhang, J. Xiao, M. Gao, N. Duan, J. Zhang, J. Li, Q. Liu, X. Yi, J.L. Luo, Wavy SnO<sub>2</sub> catalyzed simultaneous reinforcement of carbon dioxide adsorption and activation towards electrochemical conversion of CO<sub>2</sub> to HCOOH, *Appl Catal B* 261 (2020). <https://doi.org/10.1016/j.apcatb.2019.118243>.
3. F. Wei, T. Wang, X. Jiang, Y. Ai, A. Cui, J. Cui, J. Fu, J. Cheng, L. Lei, Y. Hou, S. Liu, Controllably Engineering Mesoporous Surface and Dimensionality of SnO<sub>2</sub> toward High-Performance CO<sub>2</sub> Electroreduction, *Adv Funct Mater* 30 (2020). <https://doi.org/10.1002/adfm.202002092>.
4. F. Li, L. Chen, G.P. Knowles, D.R. MacFarlane, J. Zhang, Hierarchical Mesoporous SnO<sub>2</sub> Nanosheets on Carbon Cloth: A Robust and Flexible Electrocatalyst for CO<sub>2</sub> Reduction with High Efficiency and Selectivity, *Angewandte Chemie* 129 (2017) 520–524. <https://doi.org/10.1002/ange.201608279>.
5. G. Liu, Z. Li, J. Shi, K. Sun, Y. Ji, Z. Wang, Y. Qiu, Y. Liu, Z. Wang, P.A. Hu, Black reduced porous SnO<sub>2</sub> nanosheets for CO<sub>2</sub> electroreduction with high formate selectivity and low overpotential, *Appl Catal B* 260 (2020). <https://doi.org/10.1016/j.apcatb.2019.118134>.
6. C. Liang, B. Kim, S. Yang, Y.L. Yang Liu, C. Francisco Woellner, Z. Li, R. Vajtai, W. Yang, J. Wu, P.J.A. Kenis, P.M. Ajayan, High efficiency electrochemical reduction of CO<sub>2</sub> beyond the two-electron transfer pathway on grain boundary rich ultra-small SnO<sub>2</sub> nanoparticles, *J Mater Chem A Mater* 6 (2018) 10313–10319. <https://doi.org/10.1039/C8TA01367E>.
7. S. Liu, J. Xiao, X.F. Lu, J. Wang, X. Wang, X.W. (David) Lou, Efficient Electrochemical Reduction of CO<sub>2</sub> to HCOOH over Sub-2 nm SnO<sub>2</sub> Quantum Wires with Exposed Grain Boundaries, *Angewandte Chemie International Edition* 58 (2019) 8499–8503. <https://doi.org/10.1002/anie.201903613>.
8. X. Zhou, E. Song, Z. Kuang, Z. Gao, H. Zhao, J. Liu, S. Sun, C.-Y. Mou, H. Chen, Tuning selectivity of electrochemical reduction reaction of CO<sub>2</sub> by atomically dispersed Pt into SnO<sub>2</sub> nanoparticles, *Chemical Engineering Journal* 430 (2022) 133035. <https://doi.org/10.1016/j.cej.2021.133035>.
9. D. Tan, W. Lee, K.T. Park, Y.E. Jeon, J. Hong, Y.N. Ko, Y.E. Kim, Promoting CO<sub>2</sub> reduction to formate selectivity on indium-doped tin oxide nanowires, *Appl Surf Sci* 613 (2023) 155944. <https://doi.org/10.1016/j.apsusc.2022.155944>.
10. Y. Wei, J. Liu, F. Cheng, J. Chen, Mn-doped atomic SnO<sub>2</sub> layers for highly efficient CO<sub>2</sub> electrochemical reduction, *J Mater Chem A Mater* 7 (2019) 19651–19656. <https://doi.org/10.1039/C9TA06817A>.
11. Z. Li, A. Cao, Q. Zheng, Y. Fu, T. Wang, K.T. Arul, J. Chen, B. Yang, N.M. Adli, L. Lei, C. Dong, J. Xiao, G. Wu, Y. Hou, Elucidation of the Synergistic Effect of Dopants and Vacancies on Promoted Selectivity for CO<sub>2</sub> Electroreduction to Formate, *Advanced Materials* 33 (2021). <https://doi.org/10.1002/adma.202005113>.
12. B. Zhang, L. Sun, Y. Wang, S. Chen, J. Zhang, Well-dispersed SnO<sub>2</sub> nanocrystals on N-doped carbon nanowires as efficient electrocatalysts for carbon dioxide reduction, *Journal of Energy Chemistry* 41 (2020) 7–14. <https://doi.org/10.1016/j.jechem.2019.04.022>.
13. B. Zhang, S. Chen, B. Wulan, J. Zhang, Surface modification of SnO<sub>2</sub> nanosheets via ultrathin N-doped carbon layers for improving CO<sub>2</sub> electrocatalytic reduction, *Chemical Engineering Journal* 421 (2021) 130003. <https://doi.org/10.1016/j.cej.2021.130003>.

14. S. Ning, J. Wang, D. Xiang, S. Huang, W. Chen, S. Chen, X. Kang, Electrochemical reduction of SnO<sub>2</sub> to Sn from the Bottom: In-Situ formation of SnO<sub>2</sub>/Sn heterostructure for highly efficient electrochemical reduction of carbon dioxide to formate, *J Catal* 399 (2021) 67–74. <https://doi.org/10.1016/j.jcat.2021.04.028>.
15. Y. Zhang, H. Xu, D. Niu, X. Zhang, Y. Zhang, Pyridine Grafted on SnO<sub>2</sub>-Loaded Carbon Nanotubes Acting as Cocatalyst for Highly Efficient Electroreduction of CO<sub>2</sub>, *ChemSusChem* 14 (2021) 2769–2779. <https://doi.org/10.1002/cssc.202100541>.